Title

A human monoclonal antibody neutralizes SARS-CoV-2 Omicron variants by targeting the upstream region of spike protein HR2 motif

Journal

hLife, 2(3)

ISSN

2949-9283

Authors

Su, Hang

Zhang, Jun

Yi, Zhenfei

et al.

Publication Date

2024-03-01

DOI

10.1016/j.hlife.2024.02.001

hLife

ARTICLE

A human monoclonal antibody neutralizes SARS-CoV-2 Omicron variants by targeting the upstream region of spike protein HR2 motif

Hang Su[1,2], Jun Zhang[3,4], Zhenfei Yi[1], Sajid Khan[1], Mian Peng[5], Liang Ye[1], Alan Bao[6], Han Zhang[7], Guangli Suo[8], Qian Li[3,4], Housheng Zheng[1], Dandan Wu[1], Thomas J. Kipps[9], Lanfeng Wang[3,4,*], Zhenghong Lin[2,*], Suping Zhang[1,9,*]

*Correspondence: lanfwang@ips.ac.cn (L.W.); zhenghonglin@cqu.edu.cn (Z.L.); s9zhang@szu.edu.cn (S.Z.)
Received: November 9, 2023; Revised: February 7, 2024; Accepted: February 7, 2024
Doi:10.1016/j.hlife.2024.02.001

Citation: Su H, Zhang J, Yi Z, et al. A human monoclonal antibody neutralizes SARS-CoV-2 Omicron variants by targeting the upstream region of spike protein HR2 motif. *hLife* 2024;2:126–140.

GRAPHICAL ABSTRACT

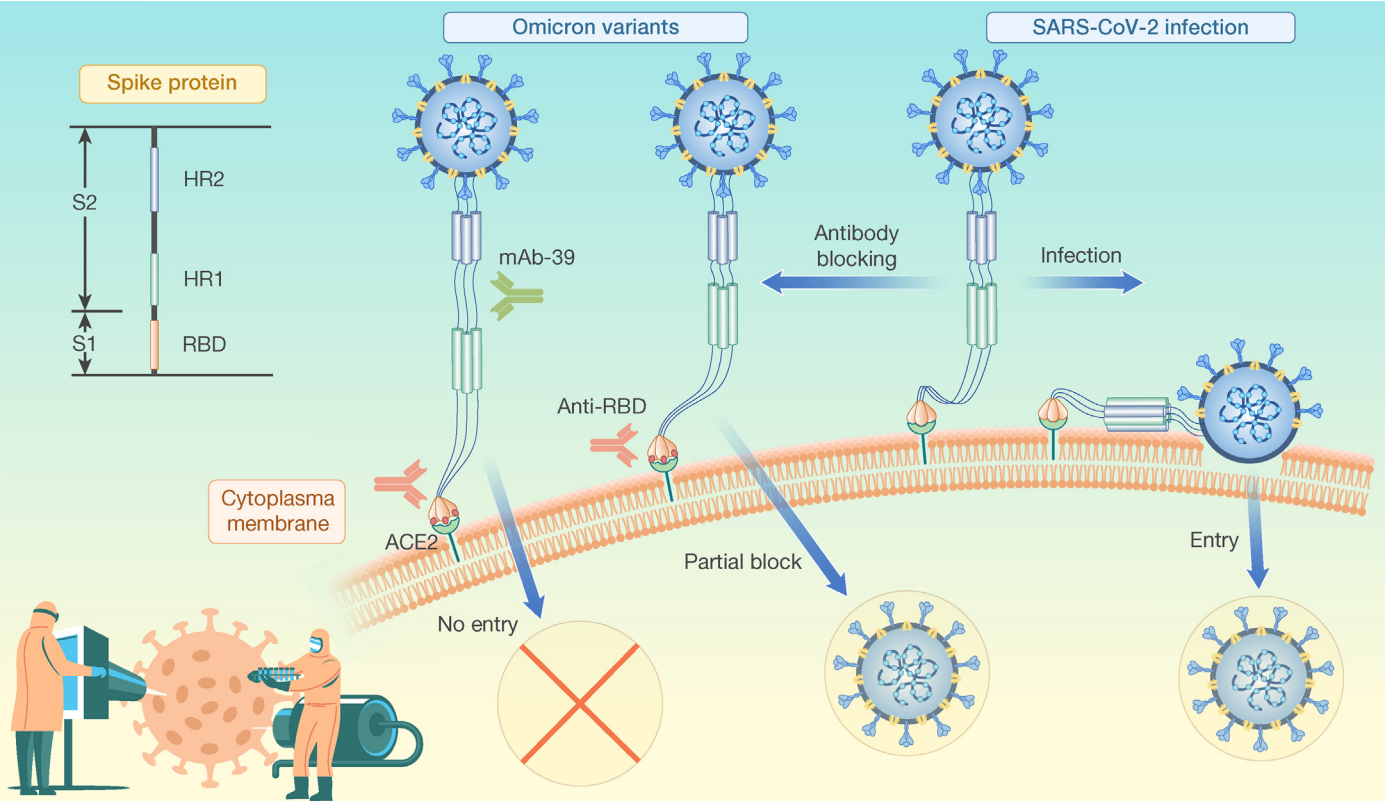

HIGHLIGHTS

- **A newly isolated human neutralizing monoclonal antibody 39 (mAb-39) can neutralize SARS-CoV-2 and its variants.**
- **mAb-39 improves the activity of anti-receptor-binding domain (anti-RBD) antibody against Omicron variants.**
- **mAb-39 binds to a conserved epitope within the upstream region of the heptad repeat 2 (HR2) motif of Omicron spike protein.**
- **Point mutation within the upstream region of HR2 reduces the capacity of spike protein-induced membrane fusion.**

A human monoclonal antibody neutralizes SARS-CoV-2 Omicron variants by targeting the upstream region of spike protein HR2 motif

Hang Su[1,2], Jun Zhang[3,4], Zhenfei Yi[1], Sajid Khan[1], Mian Peng[5], Liang Ye[1], Alan Bao[6], Han Zhang[7], Guangli Suo[8], Qian Li[3,4], Housheng Zheng[1], Dandan Wu[1], Thomas J. Kipps[9], Lanfeng Wang[3,4,*], Zhenghong Lin[2,*], Suping Zhang[1,9,*]

[1]Shenzhen Key Laboratory of Precision Medicine for Hematological Malignancies, Guangdong Key Laboratory for Genome Stability and Human Disease Prevention, Department of Pharmacology, School of Basic Medical Sciences, Base for International Science and Technology Cooperation: Carson Cancer Stem Cell Vaccines R&D Center, International Cancer Center, Shenzhen University Medical School, Shenzhen University, Guangdong, China
[2]School of Life Sciences, Chongqing University, Chongqing, China
[3]The Center for Microbes, Development and Health, CAS Key Laboratory of Molecular Virology & Immunology, Shanghai Institute of Immunity and Infection, Chinese Academy of Sciences, University of Chinese Academy of Sciences, Shanghai, China
[4]College of Life Sciences, University of Chinese Academy of Sciences, Beijing, China
[5]Department of Critical Care Medicine, Shenzhen Luohu People's Hospital, Guangdong, China
[6]University of California, Berkeley, California, USA
[7]Xenta Biomedical Science Co., Ltd, Guangdong, China
[8]CAS Key Laboratory of Nano-Bio Interface, Suzhou Institute of Nano-Tech and Nano-Bionics, Chinese Academy of Sciences, Jiangsu, China
[9]Center of Novel Therapeutics, University of California, San Diego, California, USA
*Correspondence: lanfwang@ips.ac.cn (L.W.); zhenghonglin@cqu.edu.cn (Z.L.); s9zhang@szu.edu.cn (S.Z.)
Received: November 9, 2023; Revised: February 7, 2024; Accepted: February 7, 2024
Doi:10.1016/j.hlife.2024.02.001

Citation: Su H, Zhang J, Yi Z, et al. A human monoclonal antibody neutralizes SARS-CoV-2 Omicron variants by targeting the upstream region of spike protein HR2 motif. *hLife* 2024;2:126–140.

ABSTRACT

The continuous emergence of new severe acute respiratory syndrome coronavirus 2 (SARS-CoV-2) variants means there is a need to explore additional strategies to develop broad-spectrum vaccines or therapeutics for individuals remaining at risk of coronavirus disease 2019 (COVID-19). Neutralizing monoclonal antibody (mAb) that binds to the conserved S2 subunit of the SARS-CoV-2 spike (S) protein alone, or in combination with mAb that binds to the receptor-binding domain (RBD) of S protein, might be effective in eliciting protection from infection by a variety of SARS-CoV-2 variants. Using high-throughput single-cell immunoglobulin sequencing of B cells from COVID-19-convalescent donors, we identified a high-affinity S2-specific mAb-39, that could inhibit original SARS-CoV-2 strain, Omicron BA.1, BA.2.86, BA.4, BA.5, and EG.5.1 S protein-mediated membrane fusion, leading to the neutralization of these pseudoviral infections. Moreover, mAb-39 could also improve the neutralizing activity of anti-RBD antibody against the highly neutralization-resistant Omicron variants. Molecular docking and point mutation analyses revealed that mAb-39 recognized epitopes within the conserved upstream region of the heptad repeat 2 (HR2) motif of the S2 subunit. Collectively, these findings demonstrate that targeting the conserved upstream region of the HR2 motif (e.g., using mAbs) provides a novel strategy for preventing the infection of SARS-CoV-2 and its variants.

KEYWORDS coronavirus disease 2019 (COVID-19); severe acute respiratory syndrome coronavirus 2 (SARS-CoV-2) Omicron variants; monoclonal antibody; upstream region of heptad repeat 2 (HR2); immunoglobulin repertoire sequencing

INTRODUCTION

Human coronaviruses (CoVs) are a family of enveloped, positive-sense, single-stranded RNA viruses that typically cause mild respiratory tract infections in humans [1]. However, outbreaks of infections of severe acute respiratory syndrome coronavirus (SARS-CoV), Middle East respiratory syndrome coronavirus (MERS-CoV), and more recently, SARS-CoV-2 have caused serious epidemics [2–4] and the deaths of millions of people [5–7]. Considering that continuous contact between humans and intermediate hosts and the high mutation rate of RNA

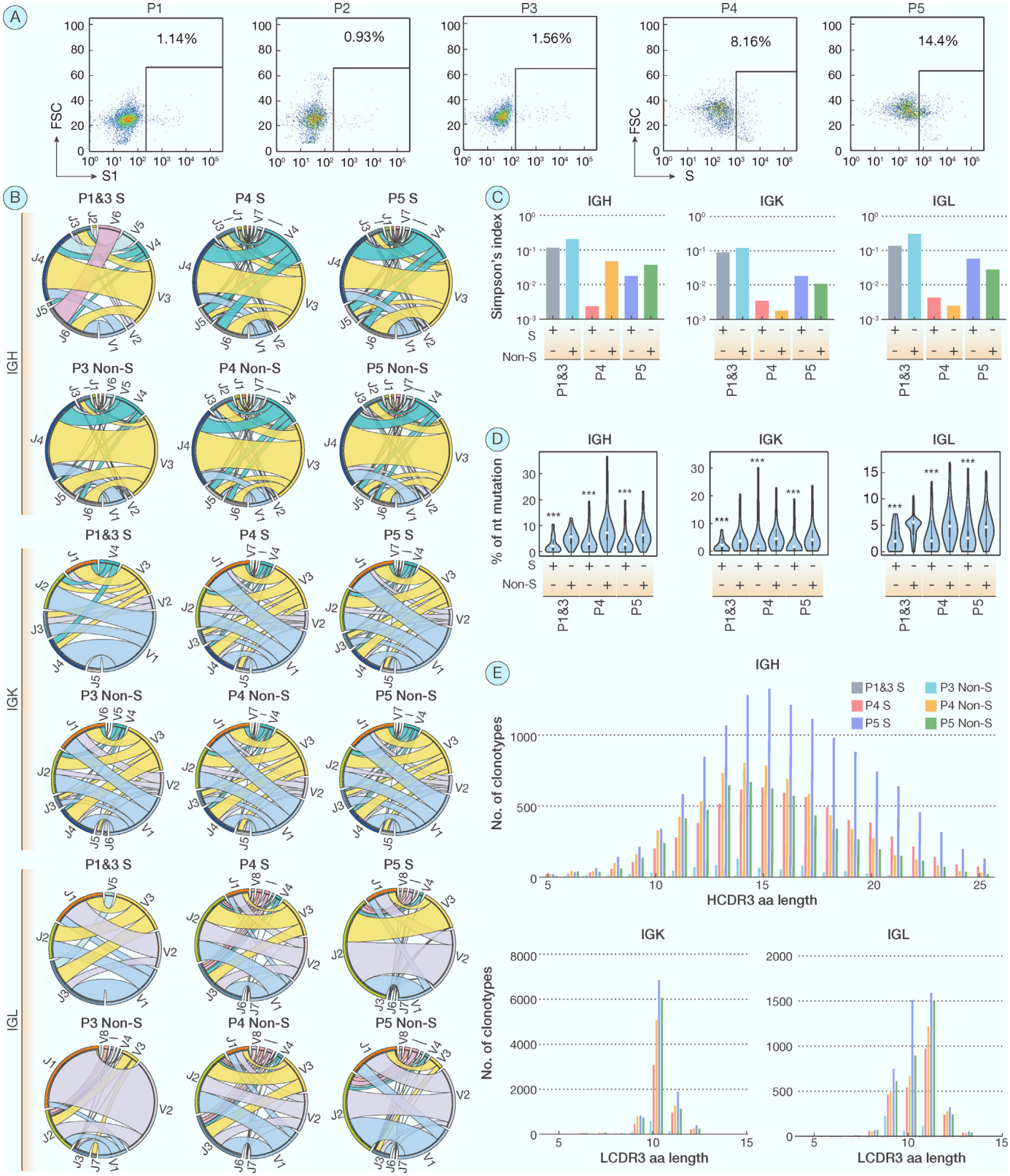

Figure 1. Characterization of the unique immunoglobulin clones for COVID-19 patients

(A) Percentage of B cells reactive to spike (S) protein or its S1 subunit (S1) in peripheral blood mononuclear cells (PBMCs) from convalescent COVID-19 patients (P1, P2, P3, P4, P5) who were infected with SARS-CoV-2 wild-type (WT) viruses was determined by FACS. (B–E) Immunoglobulin V(D)J gene of S or S1-reactive (S-reactive) *versus* non-S or S1-reactive (Non-S-reactive) B cells isolated from the convalescent COVID-19 patients were sequenced. (B) V and J gene usage of immunoglobulin in each of sequenced samples. The width of the band connecting the V and J gene families represents the frequency of the specific combination. (C) Diversity of antibody heavy and light chains in sequenced samples, as determined by Simpson's index. (D) Percentage of nucleotide (nt) mutations from the germline in the variable region of

(legend continued on next page)

viruses cause enhanced viral infectivity and immune-escape potential, currently circulating SARS-CoV-2 Omicron variants and potentially undiscovered CoVs represent threats to public health [8–12], in particular to individuals who may not have strong immune responses to the vaccine, such as elderly or immunocompromised patients [13].

A key determinant in efficient animal-to-human and human-to-human transmissions of SARS-CoV-2 is the spike (S) glycoprotein, which generally exists as a homotrimer and mediates virus entry into host cells [14,15], making it the primary target of therapeutics and vaccine development [16–18]. The S glycoprotein comprises an N-terminal S1 subunit that mediates host-cell receptor recognition and a C-terminal S2 subunit that is required for membrane fusion between the virus and the host cell [19]. The receptor-binding domain (RBD) in the S1 subunit is highly immunogenic and a key player in the viral–cell interactions mediated by angiotensin-converting enzyme 2 (ACE2) [12,20], and its sequence shows high diversity among human CoVs; hence, the most potent neutralizing antibodies (Abs) found in humans during natural CoV infections are typically raised to epitopes overlapping the ACE2-binding site [21–25]. With the rapid spread of the SARS-CoV-2 virus since late in 2019, when it was first identified, these epitopes have come under strong immune selection pressure at the population level, leading to the selection of SARS-CoV-2-neutralization-escape variants [8–10,26,27]. For example, the Omicron variant BA.1 S protein, which has the highest frequency of mutation among all variants of concern to date, harbors approximately 30 amino acid (aa) mutations, almost half of which are within the RBD [28]. These allow Omicron to evade antibody neutralization by the sera of vaccinated donors and to escape neutralization by most emergency-use authorized (EUA) therapeutic monoclonal antibodies (mAbs) [29–34]. By contrast, the S2 subunit, which consists of a fusion peptide (FP), heptad repeat1 (HR1), central helix (CH) motif, connector domain (CD), and heptad repeat 2 (HR2) [14], has a much lower frequency of mutation than the S1 subunit and exhibits a high degree of homology among human CoVs [35]. As such, the more conserved epitopes within the S2 subunit should be explored as additional targets for neutralizing mAbs that could be used alone or in combination with anti-RBD mAbs to treat patients infected with SARS-CoV-2 variants and other potential human CoVs.

Indeed, a few mAbs that target the conserved stem helix within the HR2 region of the S2 subunit elicit broad neutralizing activity against SARS-CoV-2 variants and other human CoV2, as reported recently [36–38]. However, whether targeting other regions in the S2 subunit also has anti-viral activity remains elusive. In this study, we conducted high-throughput, single-cell V(D)J sequencing to characterize the S-protein-specific immunoglobulin repertoires of convalescent COVID-19 patients. Based on this analysis, we identified a human-neutralizing antibody that targets an evolutionarily conversed upstream region of HR2 within the S2 subunit. We also examined whether this mAb alone or in combination with anti-RBD mAb can neutralize Omicron variants including those that are resistant to most therapeutic mAbs.

RESULTS

Characterization of S-specific Immunoglobulin Sequences in the Patients Infected with SARS-CoV-2

To identify S-specific antibodies, we first collected plasma and peripheral blood mononuclear cells (PBMC) samples from five Chinese convalescing patients infected with the SARS-CoV-2 wild-type (WT) strain. Enzyme-linked immunosorbent assay (ELISA) revealed that plasma from each of the convalescent patients bound to the S-trimer, S1, RBD, and S2 of the WT strain and the S-trimer of Omicron variant BA.1 (Table S1 and Figure S1A). Plasma from patients 1, 3, and 5 had a higher neutralization capacity against pseudotyped WT or Omicron BA.1 virus than plasma from patients 2 and 4, which might result from the higher antibody titers in the plasma from patients 1, 3, and 5 than that of patients 2 and 4 (Figure S1B).

We then used fluorescence-activated cell sorting (FACS) to isolate $CD19^+$ B cells specifically reactive to the extracellular domain (ECD) of the S protein (patients 4 and 5) or S1 protein from the PBMCs of patients (patients 1, 2, and 3) (Figure S2). The frequency of S-ECD-reactive B cells ranged from 8.16% to 14.4%, while the frequency of S1-specific B cells ranged from 0.93% to 1.56% (Figure 1A). We pooled the B cells that bound to the S1 protein of patients 1 and 3 (1&3) due to low cell numbers. Because SARS-CoV-2-uninfected individuals might be exposed to other seasonally spreading human CoVs, leading to the generation of antibodies against the S2 subunit [35], we isolated $CD19^+$ memory B cells that failed to bind to S-ECD or S1 protein but were IgD-negative and CD27-positive (non-S-reactive B cells) from the same convalescent patients with COVID-19, instead of $CD19^+$ B cells from healthy donors. Immunoglobulin V(D)J genes were successfully sequenced for 46, 7595, and 14,722 S-reactive B cells from patients 1&3, 4, and 5, and for 2456, 10,746, and 11,939 non-S-reactive B cells from patients 3, 4, and 5, respectively. We further analyzed the acquired immunoglobulin sequences for V and J gene usage, diversity, mutation frequency, and complementary-determining region 3 (CDR3) aa length (PRJNA820499). We found that the distribution of V in combination with J gene families was comparable among different patients and between S-reactive and non-S-reactive B cells, except for the immunoglobulin lambda light chains, where different patients displayed variable preferences for V and J gene usage. The V3-J4 combination was most commonly used in the heavy chains (Figure 1B), which is consistent with a previous study [39]. Moreover, the heavy chains, but not the light chains, of the S-reactive antibody sequences

antibody heavy and light chains in each sequenced sample. Asterisks (*) indicate the statistical significance of differences in the percent of nt mutations in heavy chain variable regions from S-reactive B cells *versus* non-S-reactive B cells in each patient. *** denotes $P < 0.001$, using Student's *t*-test. (E) Distribution of heavy-chain complementary-determining region 3 (HCDR3, upper) and light-chain complementary-determining region 3 (LCDR3, lower) aa lengths in each sequenced sample. Abbreviations: COVID-19, coronavirus disease 2019; IGH, immunoglobulin heavy chains; IGK, immunoglobulin kappa chains; IGL, immunoglobulin lambda chains; SARS-CoV-2, severe acute respiratory syndrome coronavirus 2; P1&3, P1 and P3 samples that were pooled together.

showed lower diversity compared with the non-S-reactive antibodies of B cells from the same patient, as indicated by the Simpson's index (Figure 1C), suggesting there was clonal expansion of S-specific B cells in patients who were exposed to the SARS-CoV-2 virus.

The somatic hypermutation (SHM) rates in both the heavy and light chains of antibody sequences within S-reactive B cells were also significantly lower than those in non-S-reactive B cells from the same patient (Figure 1D), implying the existence of convergent S-specific antibodies in patients with COVID-19. Conversely, the average length of the heavy-chain CDR3 (HCDR3), but not light-chain CDR3 (LCDR3), was significantly greater in S-reactive B cells compared with those in the non-S-reactive B cells ($P < 0.05$, Table S2). Conceivably, the distribution of S-reactive B cell sequences in both patients 4 and 5 was significantly biased toward longer HCDR3 but not LCDR3 compared with those of their non-S-reactive B cells (both $P < 0.001$, Figure 1E). Collectively, these observations suggest that activated B cells undergo clonal expansion in response to SARS-CoV-2 antigen exposure. This effect would lead to the generation of antibodies with long HCDR3 sequences, including convergent antibodies within patients.

Identification of an S2-specific Neutralizing mAb

The above analyses suggested the potential presence of convergent S-specific mAbs and a low diversity of S-reactive antibody sequences among patients. Thus, to identify neutralizing mAbs, we analyzed antibody sequences with an identical or similar HCDR3 differing by no more than two aa among the patients or that were present in more than one S-reactive B cell. Eleven clonally expanded antibody sequences and four antibody sequences from lineages sharing similar HCDR3 aa sequences for IgG1, along with three clones with identical HCDR3 aa sequences for non-IgG subtypes, were identified. We produced 15 IgG1 mAbs and then determined their S protein-binding capacity by ELISA. We found that 13 out of these 15 IgG1 mAbs had detectable binding activity to the S-trimer protein of the WT strain (Table S3). Notably, 2 of them derived from clonally expanded B cells of patient 5, mAb-38 (HCDR3 length: 20 aa, Table S3) and mAb-39 (HCDR3 length: 17 aa, Table S3), had strong binding capacity to the WT S-trimer (Figures 2A and S3, Table S3), while 4 mAbs within lineages sharing similar HCDR3 aa sequence (HCDR3 length: 10–12 aa) exhibited low-to-moderate binding capacity to the S-trimer protein (maximal O.D. value = 1.474, Table S3).

Further, ELISA analyses revealed that mAb-38 could bind to the non-RBD region within S1. However, mAb-39 bound to the S2 of the WT S protein, making it capable of binding to the S-trimer of Omicron BA.1, BA.2.86, BA.4, and BA.5 (BA.4 and BA.5 are hereafter referred collectively to as BA.4/BA.5), EG.5.1 (Figures 2A and S3). Biolayer interferometry analyses demonstrated that the equilibrium dissociation constants (K_D) for mAb-39 binding to the S-trimer and S2 of WT, Omicron BA.1, BA.2.86, BA.4/BA.5, and EG.5.1 were 5.55, 9.16, 0.18, 3.43, 1.13, and 0.33 nM, respectively (Figure 2B). More importantly, mAb-39 was able to inhibit WT pseudovirus infection with calculated half-maximal inhibitory concentrations (IC_{50}) of 2.00 μg/mL (Figure 3A). Despite the increased binding capacity to the S-trimer of Omicron variants, mAb-39 had relatively reduced neutralization activity against the Omicron BA.1 (IC_{50}:

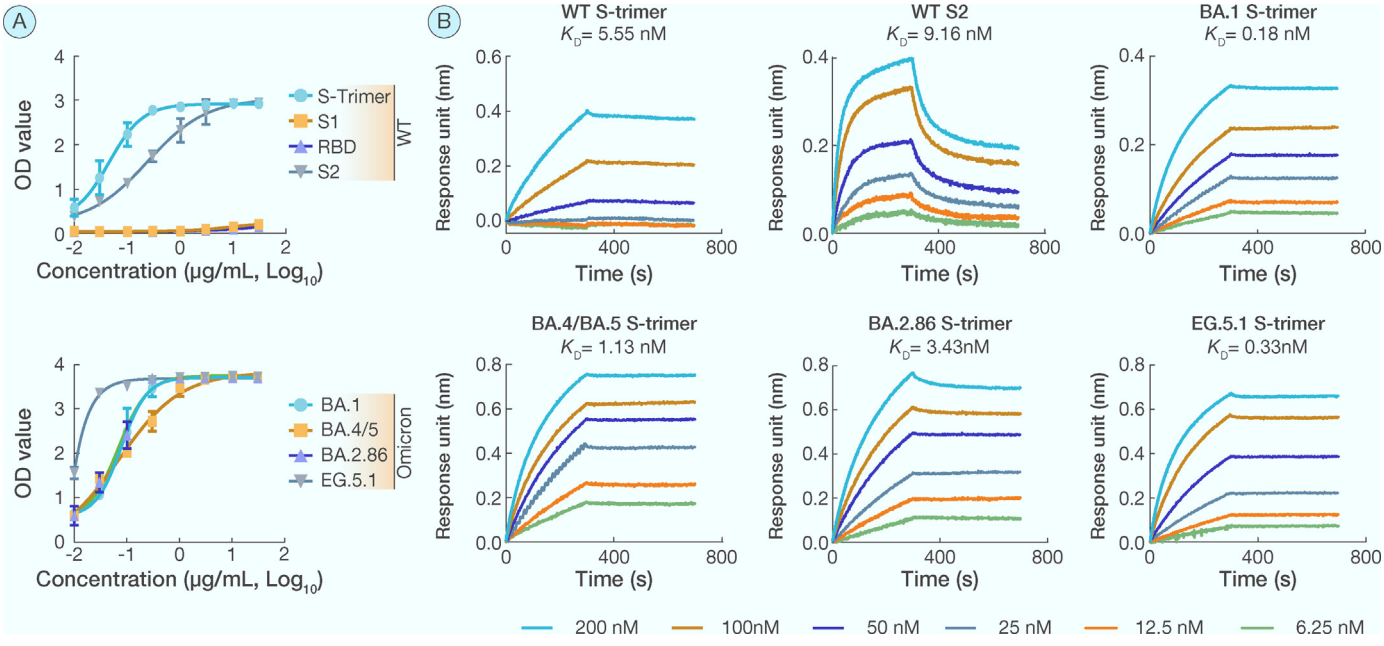

Figure 2. Binding activities of mAb-39 to S proteins of the WT and Omicron variants
(A) Binding activity of monoclonal antibody 39 (mAb-39) with increasing concentrations to the SARS-CoV-2 WT, Omicron BA.1, BA.2.86, BA.4/BA.5, and EG.5.1 trimeric S proteins (S-trimer), or S1, receptor-binding domain (RBD), S2 of the SARS-CoV-2 WT S protein as measured by ELISA. (B) Avidity and affinity measurements of mAb-39 binding to the S2 subunit of the WT strain, the S-trimer of the WT strain, Omicron BA.1, BA.2.86, BA.4/BA.5, or EG.5.1 variants, as determined by biolayer interferometry. Equilibrium dissociation constants (K_D) values are shown. Abbreviation: ELISA, enzyme-linked immunosorbent assay.

2.04 μg/mL), BA.2.86 (IC_{50}: 6.34 μg/mL), BA.4/BA.5 (IC_{50}: 3.68 μg/mL), and EG.5.1 (IC_{50}: 13.43 μg/mL) pseudovirus (Figure 3A). A cell–cell fusion assay, established by coculturing HEK293T-ACE2 cells with S-protein-expressing HEK293T cells transduced with a vector encoding GFP, further confirmed that mAb-39 at IC_{50} concentration, significantly inhibited membrane fusion mediated by the S protein of the WT, Omicron BA.1, BA.2.86, BA.4/BA.5, or EG.5.1 (Figure 3B). Taken together, these data indicate that S2-specific mAbs with long HCDR3 derived from clonally expanded B-cells in convalescent patients can neutralize pseudotyped WT or Omicron variants.

The S2-specific mAb May Improve Anti-RBD mAb Neutralization Activity Against Omicron Variants

We further examined the effect of mAb-39 in combination with the anti-RBD mAb on neutralization of Omicron variants. It appears that a commercially available neutralizing anti-RBD mAb (clone #: AM359b) could efficiently neutralize the WT and Omicron BA.1 pseudoviruses with IC_{50} of 0.19 and 0.59 μg/mL, respectively (Figure 4). However, its neutralizing activity against BA.2.86, BA.4/BA.5, or EG.5.1 pseudoviruses apparently was reduced, similar to most other anti-RBD neutralizing mAbs [40]. Notably, mAb-39 in combination with the anti-RBD mAb was more effective in neutralizing BA.2.86, BA.4/BA.5, or EG.5.1 pseudoviruses than either mAb-39 or the anti-RBD alone (Figure 4), indicating a combination of mAb-39 and the anti-RBD mAb had complementary neutralizing activity.

The Specific aa Residues Located in the Upstream Region of the HR2 Motif Comprise the Binding Epitope of the S2-specific Neutralizing mAb

To analyze the binding epitope of mAb-39 to the S protein, we performed a computational docking analysis using the electron microscopic structures of the Omicron BA.1 S-trimer with a resolution of 2.56 Å downloaded from the PDB (PDB code: 7WP9), as such protein had highest binding affinity to mAb-39 (Figure 2B). The structure of mAb-39 was predicted using MODELLER software. We found that the light and heavy chains appeared to overlap, showed considerable interaction, and bound to the same S-protein-binding pocket site (Figure 5A). Residues in both the CDR and framework regions participated in binding to the S2 subunit. For example, K1070, T1073, and N1095 of the upstream region of HR2 formed hydrogen bonds with G40, Q41, and A42 of the framework region of the mAb-39 light chain, while H1098 and F1100 in the same region formed hydrogen bonds with Y113 and G115 within CDR3 and the adjacent mAb-39 heavy chain region (Figures 5B and S4). In addition, both Y1107 and P1109 of the upstream region of the HR2 motif could also interact with Q116 and G117, which were located close in the sequence to the CDR3 of the mAb-39 heavy chain (Figures 5B and S4).

We further mutated the above residues that interacted with mAb-39 by replacing each residue with alanine (Figure 5C). We found that mAb-39 had reduced binding capacity to the Omicron BA.1 S protein mutant with K1070A and T1073A (mutation-1, ΔMFI: 5165) or N1095A, H1098A, and F1100A (mutation-2, ΔMFI: 2035) relative to the Omicron S wild-type protein (WT, ΔMFI: 7276) (Figure 5D–5E). More interestingly, mAb-39 did not bind to the Omicron BA.1 S mutant protein with Y1107A and P1109A (mutation-3, ΔMFI: 104) and had negligible binding to S protein with all five aa residues mutated in both mutation 1 and mutation 2 (mutation 1&2, ΔMFI: 154), whereas mAb-38 bound to all mutants (Figure 5E). These data indicate that all seven aa residues identified in Omicron BA.1 S protein contribute to mAb-39 binding.

Point Mutation in the Binding Epitope of S2-specific mAb-39 Reduced the Capacity of Omicron S Protein-induced Membrane Fusion

To determine the possible role of the identified epitope in virus infection, we aligned the sequence of the upstream region of the HR2 motif and found that the SARS-CoV-2 and SARS-CoV regions share 90% sequence identity, and both have the subdomain 3 (SD3) and a linker region upstream of the HR2 motif (Figure 6A). Moreover, none of mutations of the SARS-CoV-2 previous variants of concern, including Omicron subvariants BA.1, BA.2, BA.3, BA.4, BA.5, their evolved sub-lineages, and current variants of interest (e.g., EG.5.1 and BA.2.86), are located on this particular epitope (Figure 6B) [41–45], indicating this region is evolutionarily conserved. We further retrieved publicly available cryo-electron microscopy (Cryo-EM) structures of the S-trimer of SARS-CoV (6ACD), SARS-CoV-2 WT (7E5R) and Omicron BA.4/BA.5 (7YVP) from the protein data bank (PDB) and constructed the surface models that were visualized using UCSF Chimera X and PyMOL. Structure superimposition and sequence mapping analyses revealed that the upstream region of the HR2 motif of these S-trimers, in particular the SD3 region that covers the mAb-39-binding site, exhibits similar structural conformation and orientation (Figure 6C–6D). Moreover, such SD3 region of Omicron BA.1 and BA.4/BA.5 showed a larger surface area than that of SARS-CoV-2 WT (Table S4), supporting the observation of the higher binding affinity of mAb-39 to Omicron S-trimers relative to SARS-CoV-2 WT S-trimer. More importantly, GFP-transduced HEK293T cells expressing any of the above four mutations of the Omicron BA.1 S protein had a largely reduced capacity to fuse with HEK293T-ACE2 cells (Figure 6C), indicating the important role of this conserved upstream region of the HR2 motif in viral entry. Collectively, these data demonstrated that the upstream region of HR2 might serve as a target for COVID-19, and mAb-39 may disrupt membrane fusion, and thus inhibit SARS-CoV-2 cell entry, by binding to this region of the S protein.

DISCUSSION

The approach of identifying conserved surface protein targets by isolating mAbs from natural infections and utilizing their molecular information to guide immunogen design has greatly contributed to the development of therapeutics or vaccines targeting a range of complex pathogen surfaces [46–49]. In this study, we characterized the immunoglobulin repertoire specific for S-reactive B cells in convalescent patients with COVID-19, which led to the identification of the first human neutralizing mAbs that bind to a conserved upstream region of the HR2 motif within the S2 subunit of the SARS-CoV-2 S protein [50]. The synthesized mAb was able to neutralize the SARS-CoV-2 WT strain and

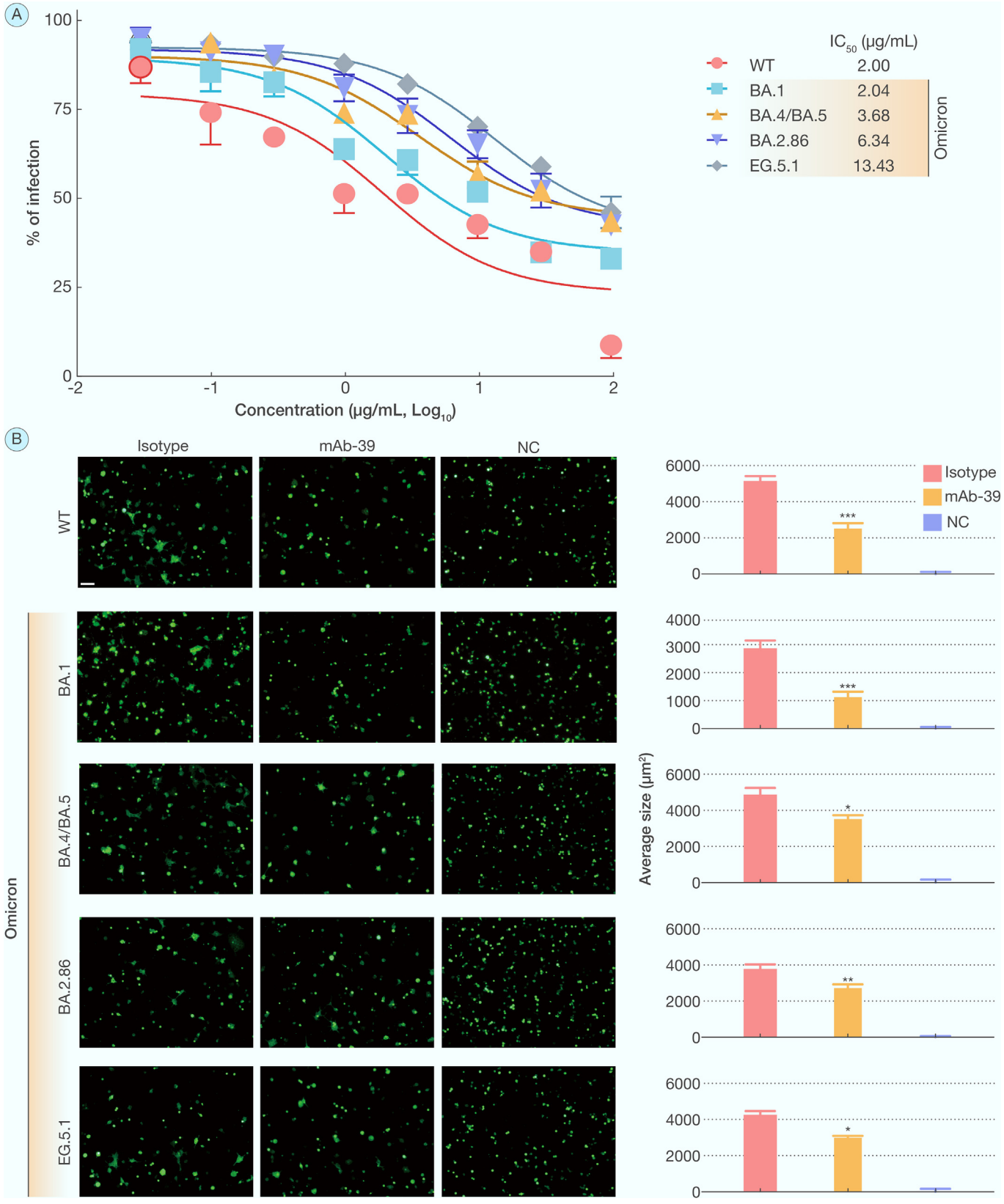

Figure 3. Neutralization activities of mAb-39 against the infections of SARS-CoV-2 WT and Omicron variants pseudovirus
(A) Neutralization activity of mAbs against the SARS-CoV-2 pseudovirus of the WT, Omicron BA.1, BA2.86, BA.4/BA.5, and EG.5.1 strains. Data represent the means ± standard error of mean (SEM) of three independent experiments. IC_{50}: half-maximal inhibitory concentrations. (B) Representative immunofluorescence images of HEK293T-ACE2 cells cocultured with green fluorescence protein (GFP)-positive cells transduced with vectors encoding the S protein of the WT strain, Omicron BA.1, BA.2.86, BA.4/BA.5, and EG.5.1 variants with or without the indicated antibodies.

(legend continued on next page)

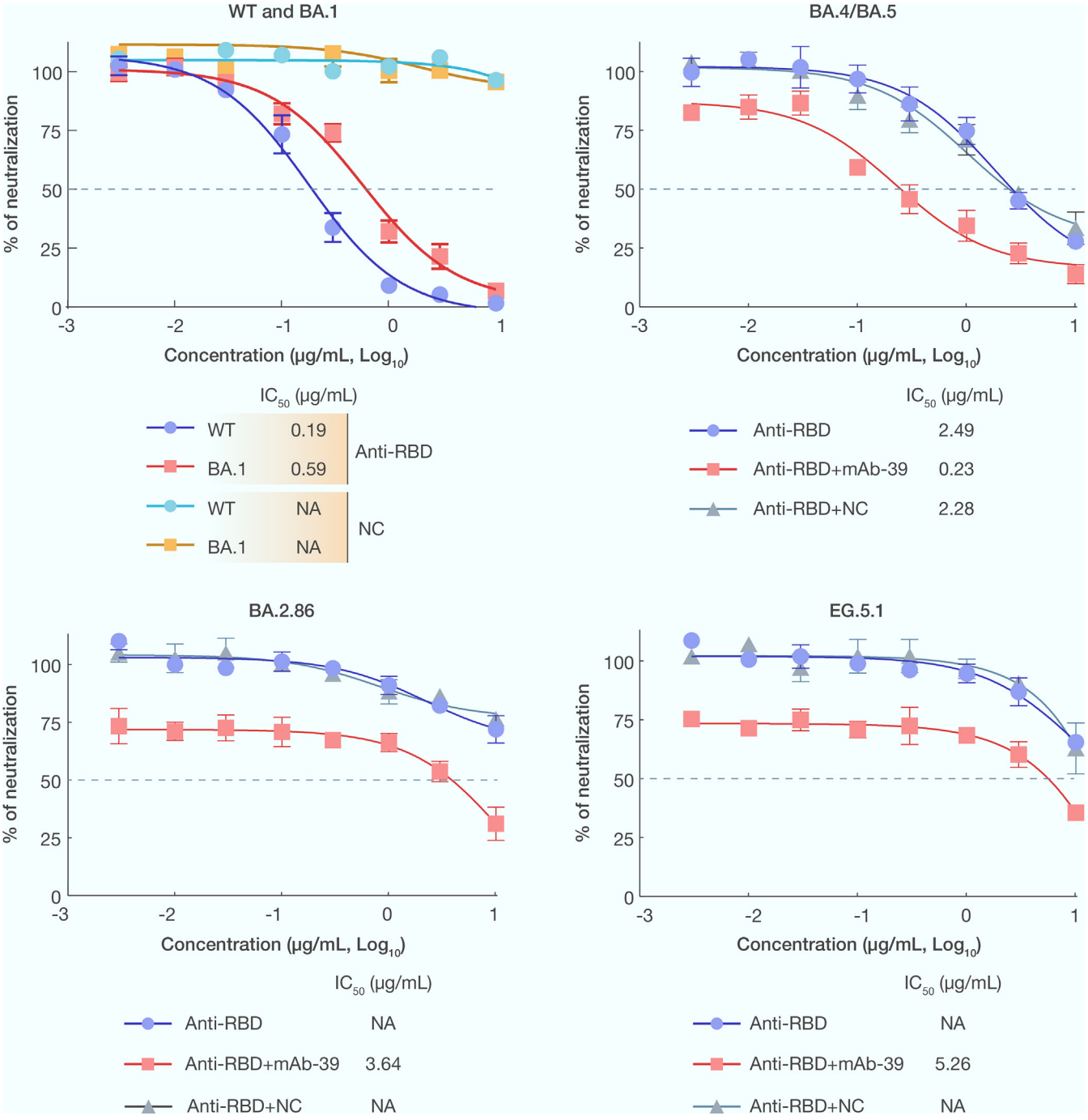

Figure 4. Neutralization activity of anti-RBD mAb alone or in combination with mAb-39 against the SARS-CoV-2 WT and Omicron variants

Neutralization activity of anti-RBD alone or in combination with mAb-39 (1 μg/mL) against the SARS-CoV-2 pseudovirus of the WT, Omicron BA.1, BA.2.86, BA.4/BA.5, and EG.5.1 strains as indicated. Data represent the means ± SEM of three independent experiments. The dashed line indicates 50% neutralizing activity, which was used to generate the IC_{50} values. Zilovertamab, specific for the receptor tyrosine kinase-like orphan receptor 1 (ROR1), serves as a negative control (NC) mAb that does not target SARS-CoV-2. Abbreviation: NA, not applicable.

Omicron BA.1, BA.2.86, BA.4/BA.5, EG.5.1, and potentially other SARS-like CoVs.

Consistent with the results of a previous study [39], we found that S-reactive B cells had a longer CDR3 sequence than non-S reactive B cells from COVID-19 patients. Interestingly, compared to the heavy chains of non-S-reactive antibodies of B cells, the heavy chain sequences of the S-reactive antibody from the same patients showed lower diversity, an observation

The bar graph depicts the average sizes of GFP-positive cells after subtracting the average sizes of HEK293T cells that expressed GFP only ± SEM. HEK293T cells that were transfected with GFP only served as a negative control (NC). Data are representative of three independent experiments. Scale bar: 100 μm * indicates $P < 0.05$; ** indicates $P < 0.01$; *** indicates $P < 0.001$, as determined by Student's *t*-test.

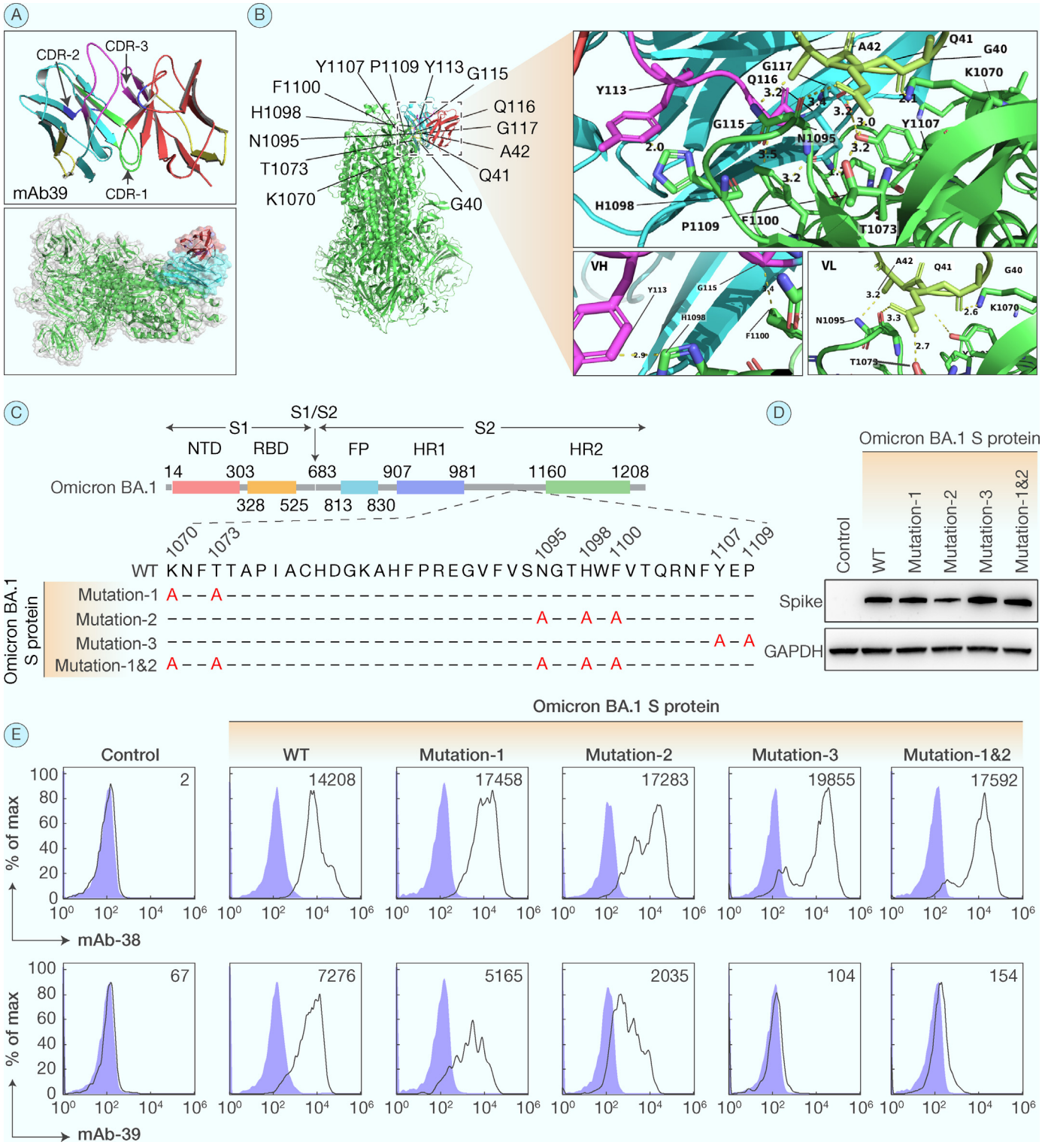

Figure 5. Identification of the S2-specific mAb-binding epitope

(A–B) Computational modeling of S-trimer (green) of the Omicron BA.1 variant complex with the light (red) and heavy (blue) chains of mAb-39. (A) Structure of mAb-39 variable region including complementary-determining region 1, 2, and 3 (CDR-1, CDR-2, CDR-3, upper), and overview of mAb-39 variable region in complex with the S-trimer of the Omicron BA.1 variant (lower). (B) Overview of S–trimer-binding epitope for mAb-39, as predicted by computational docking analysis (left). A close–up interaction view of mAb-39 binding with S-trimer is shown in the upper right panel. The aa residues in the variable light (VL) and heavy (VH) chains of mAb-39 bound to the S-trimer are shown in the lower right panels. (C) Schematic representation of extracellular domain of the wild-type (WT) or mutated S proteins of the Omicron BA.1 strain. Major domains are highlighted as colored boxes, with the start and end positions labeled. The arrow indicates the proteinase cleavage site. The lower panel shows the sequence of constructs harboring different mutations in the upstream region of the HR2 motif, which are highlighted in red. (D) Immunoblot analysis of the S protein or mutated forms from HEK293T cells transduced with empty vector or vectors encoding the S protein of Omicron BA.1 variant or its mutated forms. GAPDH served as a loading control. (E) Histograms depicting fluorescence of HEK293T cells transduced

(legend continued on next page)

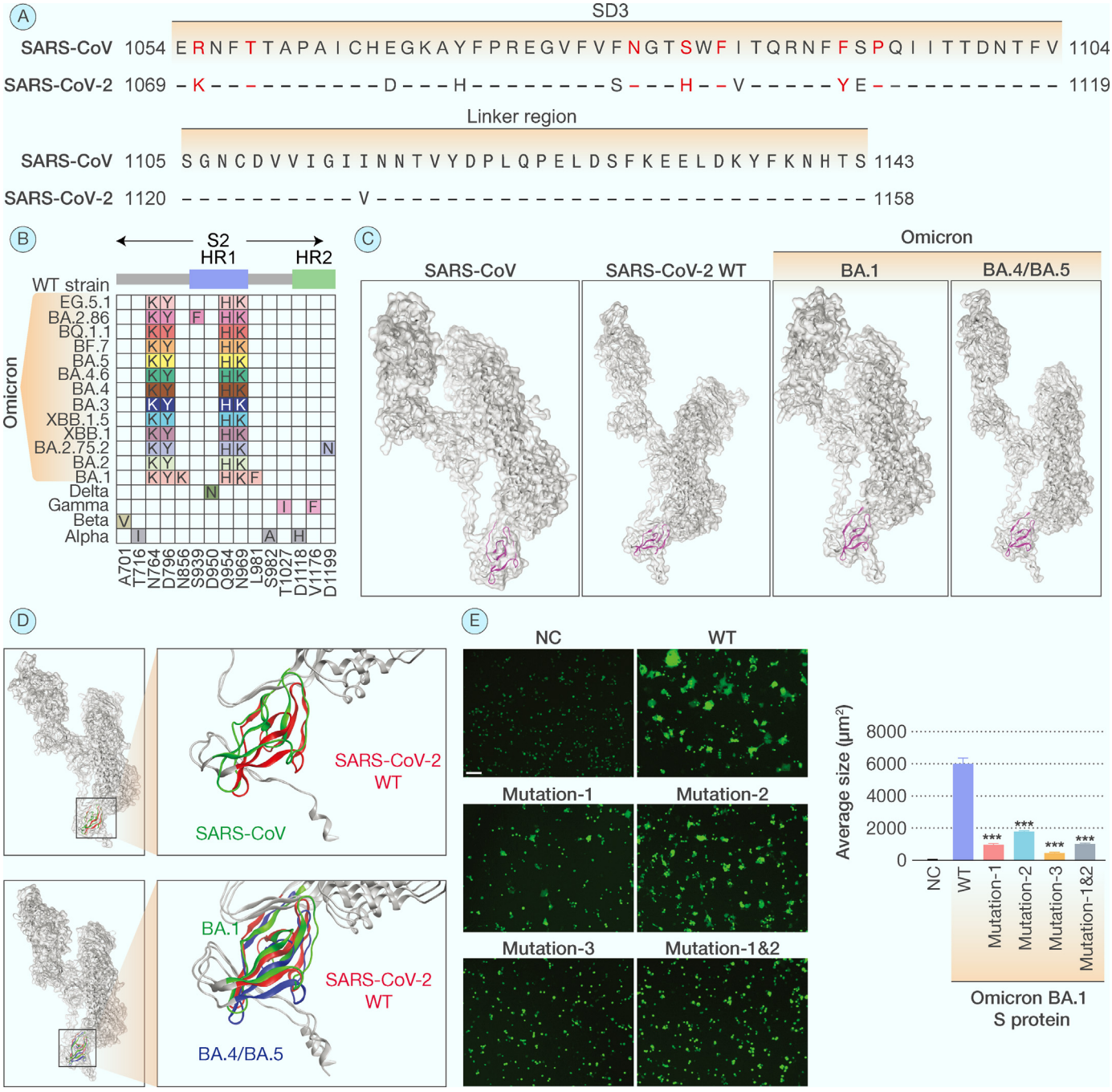

Figure 6. The epitope identified within the upstream region of the HR2 motif is necessary for Omicron membrane fusion
(A) Sequence alignment of the upstream region of the HR2 motif of SARS-CoV and SARS-CoV-2 S proteins. The identified binding site of mAb-39 is highlighted in red. (B) Schematic representation of mutations of S2 proteins from current variants of interest, previous variants of concern, and descendent lineages of Omicron variants. (C) Cryo-electron microscopy (Cryo-EM) structure surface view of the S-trimer of SARS-CoV, SARS-CoV-2 WT, Omicron BA.1, and BA.4/BA.5. SD3 region (residues 1069–1119) exposed area for mAb-39 binding was highlighted in pink magenta. (D) The superimposed surface view of the SD3 region in the SARS-CoV and SARS-CoV-2 WT (upper) and the SARS-CoV-2 WT, Omicron BA.1 and BA.4/BA.5 (lower). (E) Representative immunofluorescence images of HEK293T-ACE2 cells cocultured with GFP-positive cells transduced with empty vectors or vectors encoding WT or mutated forms of the S protein of the Omicron BA.1 variant. The bar graph depicts the average size of GFP-positive cells after subtracting the average size of HEK293T cells expressing GFP only (NC) ± SEM. Scale bar: 100 μm *$P < 0.05$; **$P < 0.01$; ***$P < 0.001$, as determined by Dunnett's multiple comparison test.

with empty vector (Control) or vectors encoding the S protein of Omicron BA.1 variant or its mutated forms stained with mAb-38 and mAb-39 (open histograms) or control mAb (shaded histogram). Numbers on the upper right corner indicate the ΔMFI that was obtained by subtracting the mean fluorescence intensity (MFI) of control mAb staining from the MFI of mAb-38 or mAb-39 staining.

supported by a prior study showing that immunoglobulin diversity was significantly reduced in COVID-19 patients compared with healthy donors [51]. These findings suggest that there is specific B-cell clonal expansion and the generation of antibodies with a long CDR3 sequence in response to SARS-CoV-2 antigen exposure, including S protein exposure. However, we found that the SHM rates in antibody sequences derived from S-reactive B cells were significantly lower than those in non-S-reactive B cells from the same patient, which is a different result than that obtained in previous analyses of sorted S-reactive B cells from convalescent patients and healthy donors demonstrating that natural SARS-CoV-2 infection elicits high levels of SHM in memory B cells [39]. This discrepancy might be due to interference from pre-existing S2 antibodies with cross-reactivity in healthy donors [35], warranting the possible development of a convergent, naturally existing S2 antibody from SARS-CoV-2-uninfected and -infected individuals.

The formulation of most of the current therapeutic antibodies used for treating patients with COVID-19 has focused on the poorly conserved RBD domain of the S1 subunit [52]. Although a few S2-specific mAbs identified to date have also exhibited neutralization activity, the specific binding regions of most were not characterized, except for a few neutralizing mAbs targeting the conserved stem helix within the HR2 region of the S2 subunit of SARS-CoV-2 [36–38,53,54]. S2-neutralizing mAb-39 specifically recognizes an upstream region of the HR2 motif, given that the substitution of aa residues with alanine completely abolished the binding capacity of mAb-39 to the S protein. Moreover, none of the mutations of SARS-CoV-2 previous variants of concern and current variants of interest, including Omicron variants, occur within this particular epitope [40,41], which is why mAb-39 exhibits broad neutralization activity against Omicron variants. However, compared with SARS-CoV-2 WT, Omicron variants (e.g., EG.5.1) have a reduced fusogenicity [55,56], which might account for the relatively decreased neutralization activity of mAb-39 against Omicron variants.

The upstream region of the HR2 motif might serve as a target for broad-spectrum vaccine and drug development for SARS-like CoVs, given that this region exhibits high homology between SARS-CoV-2 and SARS-CoV. According to previous post-fusion structural analyses on the SARS-CoV S protein, the SD3 region might be involved in retaining protein structures upon cleavage of S1/S2. Then, the linker region upstream of the HR2 motif is released and can extend along the axis of the stem helix to form a six-helix bundle, which mediates fusion between the viral and host membranes [57]. Mutations at aa residues K1070, T1073, N1095, H1098, and F1100 or Y1107 and P1109 located in the SD3 region (aa: 1069–1119) of the Omicron BA.1 S protein abolished S protein-induced fusion, indicating the essential role of the upstream region of the HR2 motif in the fusion process. Therefore, binding of mAb-39 to this region might destabilize the S2 subunit structure, prevent the linker loop from binding along the CH, and subsequently block the association between the HR2 motif and the HR1 helices in the late stages of membrane fusion. Consistent with this hypothesis, a mAb targeting the HR2 upstream linker region of SARS-CoV conferred cross-protection against viral entry mediated by the S proteins of human, civet, and bat SARS-CoVs [58,59], suggesting that targeting the upstream region of the HR2 motif might prevent infection by SARS-like CoVs.

Antibody cocktails are effective in preventing the neutralization escape of highly mutated SARS-CoV-2 variants by targeting multiple viral epitopes [60]. FDA-proved EUA antibody cocktails were two mAbs that bind distinct and non-overlapping regions of the RBD and thus can simultaneously bind to RBD and block RBD function [61]. We found that a combination of two mAbs distinctively targeting RBD and S2 that are responsible for two different critical steps of viral entry: viral binding and viral fusion, respectively, also could have enhanced neutralizing activity against SARS-CoV-2 variants such as Omicron BA.2.86, BA.4/BA.5, or EG.5.1, the variants that exhibit neutralization escape from COVID-19-vaccinated serum [45,62,63]. We speculate that S2-specific neutralizing mAbs (e.g., mAb-39) could be added to antibody cocktail therapeutics to treat COVID-19, to improve therapeutic efficacy, and to avoid viral escape from the mAbs.

Overall, this study revealed that the conserved upstream region of the HR2 motif within the S2 subunit might serve as a potential target for patients with COVID-19, and S2-specific mAb-39 alone or in combination with anti-RBD mAb could elicit protection from infection of SARS-CoV-2 WT and Omicron variants. As the identification of the novel neutralizing sites could lead to the development of efficacious vaccines based on peptide mimics of the epitopes, subunit vaccine candidates derived from the conserved neutralizing epitopes identified in this study and/or other studies [36,38], could be designed and tested in animal models for potential usage in the prevention of SARS-like CoV infection.

MATERIALS AND METHODS

Human Participants

This study was performed in compliance with the Declaration of Helsinki and approved by the Ethics Committee of Shenzhen University, China. Peripheral blood was drawn from five convalescent patients following infection with COVID-19 who were discharged from Shenzhen Third People's Hospital. All participants provided signed informed consent. Plasma was separated from peripheral blood, and PBMCs were isolated by density-gradient centrifugation with Lymphoprep (Stemcell, Vancouver, Canada) in 50 mL Sepmate tubes (Stemcell, Vancouver, Canada).

Flow Cytometry Analysis

To isolate S-reactive B cells, the ECD of S (Genscript, Jiangsu, China) or S1 (in-house) protein of WT SARS-CoV-2 was conjugated to phycoerythrin (PE) using a PE/R-Phycoerythrin Conjugation Kit – Lightning-Link (Abcam, Cambridge, UK), according to the manufacturer's instructions. PBMCs isolated from each of the convalescent patients were re-suspended in FACS buffer (phosphate-buffered saline [PBS] containing 4% fetal bovine serum [FBS]), then blocked with human Fc-block reagent (BioLegend, California, USA) for 10 min prior to staining with S- or S1-PE, phycoerythrin-cyanine7-conjugated anti-CD19 (Biolegend, California, USA), allophycocyanin-conjugated anti-CD27 (Biolegend, California, USA), and fluorescein

isothiocyanate-conjugated anti-IgD (Biolegend, California, USA) for 20 min on ice. Then, the cells were washed three times with FACS buffer and stained with 7-aminoactinomycin D (7-AAD, BD Biosciences, New Jersey, USA). Forward light scatter and side-light scatter gating were used to exclude cell debris. Cells that were 7AAD-positive were also excluded from viable cell analysis. CD19-positive ($CD19^+$) B cells that were reactive to S1 or S were gated as S-reactive B cells. $CD19^+$ cells that failed to react with S1 or S but were IgD-negative and CD27-positive were designated non-S-reactive memory B cells. Data were acquired using a FACS Aria III flow cytometer (BD Biosciences, New Jersey, USA).

HEK293T cells were purchased from the American Type Culture Collection (Manassas, Virginia, USA) and maintained free of mycoplasma in DMEM (HyClone, Utah, USA) plus 10% FBS (HyClone, Utah, USA). To determine mAb-39-binding activity to S proteins with different mutations, an empty expression vector or vectors encoding WT or mutant forms of Omicron BA.1 S protein were transfected into HEK293T cells using Lipofectamine 3000 reagent (Thermo Fisher Scientific, Massachusetts, USA). The cells were harvested 48 h post-transfection and stained with mAb-39 for 45 min on ice. The cells were then washed three times with PBS before being incubated with Alexa Fluor 647-labeled goat anti-human IgG (Thermo Fisher Scientific, Massachusetts, USA) for 30 min on ice. After being washed three times with PBS, the cells were stained with propidium iodide to exclude dead cells. Data were acquired using a flow cytometer (Attune NxT, Thermo Fisher Scientific, Massachusetts, USA) and analyzed using FlowJo 10.7.1.

Single-cell Sequencing and Immunoglobulin Repertoire Analysis

Single-cell V(D)J libraries were prepared using the 10x Chromium system following the instructions provided with Chromium Next GEM Single Cell V(D)J Reagent Kits v1.1 (10X Genomics, California, USA). Briefly, sorted cells were loaded into a Chromium Controller and mixed with Single Cell 5′ Gel Beads to generate barcoded droplets, followed by reverse transcription and cDNA amplification. After a cleanup step, full-length immunoglobulin segments were enriched using the Single Cell V(D)J Enrichment Kit for Human B Cells (10X Genomics, California, USA). Enriched libraries were constructed using a Single Cell 5′ Library Construction Kit and indexed, followed by sequencing on an Illumina NovaSeq 6000. Raw data processing, including quality control, V(D)J gene assembly and annotation, and clonotype analysis, was performed using Cell Ranger (3.0.2). The metrics of clonotype diversity and the distribution of the CDR3 length of the immunoglobulin repertoire were computed using the R software package "immunarch" (https://immunarch.com). V and J gene usage and their combination and germline mutation distance analyses were generated using in-house scripts. The sequencing data were deposited in the NCBI Sequence Read Archive database (Accession ID: PRJNA820499).

Antibody Production

Variable regions of each pair of heavy and light chains were cloned into expression vectors containing the human IgG1 constant region and transfected into Chinese Hamster Ovary cells (Gibco, Massachusetts, USA) using the ExpiCHO Expression System (Gibco, Massachusetts, USA). Supernatants were harvested 7 days post-transfection and passed three times through a column filled with protein A (Bestchrom Biosciences, Shanghai, China). Bound antibodies were then eluted using 0.1 M glycine buffer (pH 3.0), collected in 1 M Tris–HCl buffer (pH 8.0), and buffer-exchanged with PBS by ultrafiltration.

Enzyme-linked Immunosorbent Assay Screening for Plasma and Antibodies

Polybrene ELISA plates were coated overnight with 2 μg/mL SARS-CoV-2 the trimeric S (S-trimer) (Crystalo Biopharma, Shenzhen, China); the S1, RBD (Oukai Biotechnology, Jiangsu, China), or S2 (SinoBiological, Beijing, China) of the WT strain (NCBI Reference Sequence: YP_009724390.1); S-trimer of the Omicron BA.1 (Novoprotein, Jiangsu, China), BA.2.86, EG.5.1 or BA.4/BA.5 (SinoBiological, Beijing, China) dissolved in PBS. After three washes with PBS containing 0.05% Tween 20 (PBST), the plates were blocked with 150 μL PBST containing 5% milk per well for 1.5 h at room temperature (RT). The plates were then washed three times with PBST and incubated with serially diluted antibodies or plasma from convalescent patients with COVID-19 as indicated for 1 h and 45 min at RT. After three washes with PBST, horseradish peroxidase (HRP)-conjugated goat anti-human IgG (H + L) (Proteintech, Illinois, USA) was added and incubated for 1 h 20 min at RT. After a final wash, 100 μL of 3,3′,5,5′-tetramethylbenzidine (4A Biotech, Beijing, China) was added to serve as a substrate, as per the manufacturer's recommendations. The absorbance at 450 nm was measured using a microplate reader. The data were analyzed using GraphPad Prism 7.0.

Biolayer Interferometry Binding Assays

The binding affinities of mAb-38 and -39 with the S-trimer were measured by biolayer interferometry on an Octet-Red 96 system using streptavidin-coated biosensors (FortéBio, California, USA). The following four-step sequential assay was then performed at 25 °C. First, samples and buffer were added to 96-well plates, and 10 μg/mL mAb-38 or -39 diluted with PBS plus 0.02% Tween 20 was loaded onto Octec AHC-biosensors (Sartorius, Göttingen, Germany). The AHC-coated biosensors were then dipped into PBS with 0.02% Tween 20 for 150 s to reach the baseline conditions, before being incubated with 2-fold serially diluted antigens in PBS with 0.02% Tween-20 for association and PBS with 0.02% Tween 20 only for dissociation. The data were analyzed with FortéBio Data Analysis software, and a 1:1 binding model was used.

Pseudovirus Neutralization

Pseudoviruses were produced by co-transfecting plasmids encoding the SARS-CoV-2 S protein of either the WT strain (NCBI Reference Sequence: YP_009724390.1), Omicron BA.1 (IGe Biotechnology, Guangdong, China) with a reporter vector encoding luciferase, as well as RSV-REV and pMDL g/p RRE vectors, into HEK293T cells using a calcium phosphate transfection kit (Invitrogen, Massachusetts, USA) according to the

manufacturer's instructions. Supernatants containing viruses were harvested at 48 h and 72 h post-transfection. Pseudoviruses of BA.2.86, BA.4/BA.5, and EG.5.1 variants were purchased from Genomeditech, Shanghai, China.

To perform the pseudovirus neutralization assay, pLVX-hACE2 constructs were purchased from Hedgehog BioScience and Technology (Shanghai, China) and transfected into HEK293T cells to generate cells that stably expressed the human ACE2 receptor (HEK293T-ACE2). Then, the HEK293T-ACE2 cells were seeded into 96-well plates at a density of 12,000 cells per well and cultured overnight at 37 °C. Pseudoviruses with or without serially diluted antibodies or plasma were incubated for 1 h at 37 °C before being added to the wells. At 24 h post-infection, the supernatants were removed, and the cells were washed with PBS. The luciferase activity in each well was measured using a luciferase assay system (Promega, Wisconsin, USA), according to the manufacturer's instructions. The values were plotted by fitting to a nonlinear regression model, and the 50% neutralization dose was calculated using GraphPad Prism 7. Zilovertamab (formerly called cirmtuzumab) specific for the receptor tyrosine kinase-like orphan receptor 1 (ROR1) serves as a negative control (NC) mAb that does not target SARS-CoV-2 [64].

Cell–cell Fusion Assay

HEK293T-ACE2 cells were seeded at 10,000 cells per well into a 96-well plate. HEK293T cells were transfected with plasmids encoding the S protein of the WT strain, Omicron BA.1, BA.2.86, EG.5.1, BA.4/BA.5, or mutated forms of Omicron BA.1 S protein together with plasmids encoding a green fluorescent protein (GFP) using Lipofectamine 3000 reagent. HEK293T cells that were transfected with GFP only served as a negative control (NC). Cells that were transfected with constructs encoding different S protein sequences were harvested and incubated with HEK293T-ACE2 cells for 8 h with or without pre-incubation with indicated antibodies for 1 h at 37 °C. Fluorescent images were captured under a fluorescent microscope (Olympus, Tokyo, Japan) and processed using ImageJ software. The average size of GFP-positive cells was calculated, followed by subtracting the average size of HEK-293T cells transfected with GFP only.

In Silico Structural Modeling and Docking Analysis

An ERRAT score [65], VERIFY 3D [66], and Ramachandran plots [67] were used to validate the mAb-39 structure, which was modeled using MODELLER software [68] and validated using SAVES software (http://nihserver.mbi.ucla.edu/SAVES). Then, the Cryo-EM structures of the S-trimer protein of SARS-CoV (6ACD), SARS-CoV-2 WT (7E5R), Omicron BA.1 (7WP9), and Omicron BA.4/5 (7YVP), were retrieved from the PDB. The surface models were constructed and visualized using UCSF ChimeraX (www.rbvi.ucsf.edu/chimerax) and PyMOL (http://www.pymol.org). The PyMOL command line was utilized to calculate the entire surface area of the S-trimer and the specific surface area of the SD3 region (residues 1069–1119).

The hydrogen-dock server (http://hdock.phys.hust.edu.cn/) was used to perform molecular docking analysis of the antibody and Omicron BA.1 S-trimer after eliminating superfluous chains of ligand molecules and reducing energy. S-trimer protein–antibody complexes with the best docking scores and energy values were considered. PyMOL was used to conduct further interaction analysis of the protein–antibody interactions. All docking complexes showed hydrogen-bonding (acceptor, donor) and hydrophobic interactions with the receptor residue.

Immunoblot Analysis

Cells were lysed in radioimmunoprecipitation assay buffer (Applygen, Beijing, China) containing a protease and phosphatase inhibitor cocktail for 30 min on ice. The protein lysates were resolved by sodium dodecyl sulfate polyacrylamide gel electrophoresis and transferred to polyvinylidene fluoride membranes. After blocking with 5% non-fat milk, the membranes were incubated with mouse anti-S (NanJing Livingchip Biotechnology Co., Ltd, Jiangsu, China) and anti-GAPDH (Proteintech, Hubei, China) antibodies overnight at 4 °C. The membranes were then incubated with HRP-conjugated anti-mouse IgG antibody (Cell Signaling Technology, Massachusetts, USA) and detected with ECL reagent (Millipore, Massachusetts, USA). Protein bands were visualized using a Tanon-5200 Automatic Chemiluminescence Imaging Analysis System (Tanon, Shanghai, China).

Statistical Analysis

Statistical significance between two groups was determined via Student's *t*-test and differences among multiple groups were determined by Dunnett's multiple comparison tests using GraphPad Prism 7. The two-sample Kolmogorov–Smirnov test was used to compare CDR3 distributions between S-reactive and non-S-reactive immunoglobulin sequences by SPSS Statistics software (version 25). P values < 0.05 were considered statistically significant.

ETHICS APPROVAL

The study was conducted according to the guidelines of the Declaration of Helsinki and approved by the Institutional Review Board of Shenzhen University (IRB no.PN-202200064). Informed consent was obtained from all subjects involved in the study.

DATA AVAILABILITY

The single-cell immunorepertoire sequencing data were deposited in the NCBI sequence Read Archive database (Accession ID: PRJNA820499).

ACKNOWLEDGMENTS

The authors would like to thank Dr. Hu Zhou (Xiamen University, Fujian, China) for providing the construct encoding the S protein of the WT strain; Dr. Guangli Suo (Suzhou Institute of Nano-Tech and Nano-Bionics [SINANO]), Chinese Academy of Sciences, Zhejiang, China) for providing the S1 protein; Yinan Huang, Dr. Ke Wang and Na Zhu (Shenzhen University) for technical help with the characterization of the expression vector encoding different proteins and/or mAbs production; and Dr Jessica Tamanini (Shenzhen University, ET editing) for editing the paper prior to submission. This research was funded by the National Natural Science Foundation of China (81972753, 32170712, and 32170937); R&D Program of Guangzhou National Laboratory (SRPG22-003); the China Postdoctoral

Science Foundation (2019M663093); Prevention and Control of COVID-2019 Research Program in University of Guangdong Province (2020KZDZX1176); the Science and Technology Program of Guangdong Province, China (2020A1515110410 and 2021A1515010917); the Guangdong Medical Science and Technology Research Foundation (A2021336); Shenzhen Key Laboratory Foundation (ZDSYS20200811143757022); the Shenzhen Science and Technology Basic Research Program (JCYJ20180507182203049 and JCYJ20230807142815034); and the Shenzhen University (SZU) Top Ranking Project (86000000210).

AUTHOR CONTRIBUTIONS

Hang Su: writing – original draft, visualization, investigation, funding acquisition. **Jun Zhang**: visualization, investigation. **Zhenfei Yi**: investigation. **Sajid Khan**: visualization, software, investigation. **Mian Peng**: resources. **Liang Ye**: writing – review & editing, methodology, funding acquisition. **Alan Bao**: visualization, software, investigation. **Han Zhang**: writing – review & editing, resources, methodology. **Guangli Suo**: resources. **Qian Li**: investigation. **Housheng Zheng**: investigation. **Dandan Wu**: investigation. **Thomas J. Kipps**: writing – review & editing, methodology. **Lanfeng Wang**: writing – review & editing, supervision, methodology, conceptualization. **Zhenghong Lin**: supervision, conceptualization. **Suping Zhang**: writing – original draft, supervision, methodology, funding acquisition, conceptualization.

DECLARATION OF COMPETING INTEREST

The authors declare that they have no known competing financial interests or personal relationships that could have appeared to influence the work reported in this paper.

SUPPLEMENTARY DATA

Supplementary data to this article can be found online at https://doi.org/10.1016/j.hlife.2024.02.001.

REFERENCES

[1] Su S, Wong G, Shi W, Liu J, Lai ACK, Zhou J, et al. Epidemiology, genetic recombination, and pathogenesis of coronaviruses. *Trends Microbiol* 2016;24:490–502.
[2] Li J, Lai S, Gao GF, Shi W. The emergence, genomic diversity and global spread of SARS-CoV-2. *Nature* 2021;600:408–18.
[3] Peiris JS, Guan Y, Yuen KY. Severe acute respiratory syndrome. *Nat Med* 2004;10:S88–97.
[4] Durai P, Batool M, Shah M, Choi S. Middle East respiratory syndrome coronavirus: transmission, virology and therapeutic targeting to aid in outbreak control. *Exp Mol Med* 2015;47:e181.
[5] World Health Organization. *Summary of probable SARS cases with onset of illness from 1 November 2002 to 31 July 2003* (2023). https://www.who.int/publications/m/item/summary-of-probable-sars-cases-with-onset-of-illness-from-1-november-2002-to-31-july-2003.
[6] Donnelly CA, Malik MR, Elkholy A, Cauchemez S, Van Kerkhove MD. Worldwide reduction in MERS cases and deaths since 2016. *Emerg Infect Dis* 2019;25:1758–60.
[7] World Health Organization. *Number of COVID-19 cases reported to WHO* (2023). https://covid19.who.int/?gclidAIaIQobChMIht_qyL_K6gIVB7tCh2AIgwMEAAYASAAEgLyX_D_BwE/.0.
[8] Davies NG, Abbott S, Barnard RC, Jarvis CI, Kucharski AJ, Munday JD, et al. Estimated transmissibility and impact of SARS-CoV-2 lineage B.1.1.7 in England. *Science* 2021;372:eabg3055.
[9] Li B, Deng A, Li K, Hu Y, Li Z, Shi Y, et al. Viral infection and transmission in a large, well-traced outbreak caused by the SARS-CoV-2 Delta variant. *Nat Commun* 2022;13:460.
[10] Araf Y, Akter F, Tang YD, Fatemi R, Parvez MSA, Zheng C, et al. Omicron variant of SARS-CoV-2: genomics, transmissibility, and responses to current COVID-19 vaccines. *J Med Virol* 2022;94:1825–32.
[11] Mlcochova P, Kemp SA, Dhar MS, Papa G, Meng B, Ferreira IATM, et al. SARS-CoV-2 B.1.617.2 delta variant replication and immune evasion. *Nature* 2021;599:114–9.
[12] Zhou P, Yang XL, Wang XG, Hu B, Zhang L, Zhang W, et al. A pneumonia outbreak associated with a new coronavirus of probable bat origin. *Nature* 2020;579:270–3.
[13] Pashaei M, Rezaei N. Immunotherapy for SARS-CoV-2: potential opportunities. *Expet Opin Biol Ther* 2020;20:1111–6.
[14] Cai Y, Zhang J, Xiao T, Peng H, Sterling SM, Walsh Jr RM, et al. Distinct conformational states of SARS-CoV-2 spike protein. *Science* 2020;369:1586–92.
[15] Shang J, Wan Y, Luo C, Ye G, Geng Q, Auerbach A, et al. Cell entry mechanisms of SARS-CoV-2. *Proc Natl Acad Sci USA* 2020;117:11727–34.
[16] Hwang YC, Lu RM, Su SC, Chiang PY, Ko SH, Ke FY, et al. Monoclonal antibodies for COVID-19 therapy and SARS-CoV-2 detection. *J Biomed Sci* 2022;29:1.
[17] Migo W, Boskovic M, Likic R. The development of biologics to target SARS-CoV2: treatment potential of antibodies in patient groups with poor immune response. *Curr Res Pharmacol Drug Discov* 2021;2:100064.
[18] Sharma A, Sharma RP, Kaur R, Sharma R, Singh S. A comprehensive insight on the COVID-19 vaccine candidates. *J Fam Med Prim Care* 2021;10:2457–66.
[19] Huang Y, Yang C, Xu XF, Xu W, Liu SW. Structural and functional properties of SARS-CoV-2 spike protein: potential antivirus drug development for COVID-19. *Acta Pharmacol Sin* 2020;41:1141–9.
[20] Yan R, Zhang Y, Li Y, Xia L, Guo Y, Zhou Q. Structural basis for the recognition of SARS-CoV-2 by full-length human ACE2. *Science* 2020;367:1444–8.
[21] Robbiani DF, Gaebler C, Muecksch F, Lorenzi JCC, Wang Z, Cho A, et al. Convergent antibody responses to SARS-CoV-2 in convalescent individuals. *Nature* 2020;584:437–42.
[22] Rogers TF, Zhao F, Huang D, Beutler N, Burns A, He WT, et al. Isolation of potent SARS-CoV-2 neutralizing antibodies and protection from disease in a small animal model. *Science* 2020;369:956–63.
[23] Wang Z, Schmidt F, Weisblum Y, Muecksch F, Barnes CO, Finkin S, et al. mRNA vaccine-elicited antibodies to SARS-CoV-2 and circulating variants. *Nature* 2021;592:616–22.
[24] Yuan M, Liu H, Wu NC, Lee CD, Zhu X, Zhao F, et al. Structural basis of a shared antibody response to SARS-CoV-2. *Science* 2020;369:1119–23.
[25] Barnes CO, West Jr AP, Huey-Tubman KE, Hoffmann MAG, Sharaf NG, Hoffman PR, et al. Structures of human antibodies bound to SARS-CoV-2 spike reveal common epitopes and recurrent features of antibodies. *Cell* 2020;182:828–842.e16.
[26] Tegally H, Wilkinson E, Giovanetti M, Iranzadeh A, Fonseca V, Giandhari J, et al. Detection of a SARS-CoV-2 variant of concern in South Africa. *Nature* 2021;592:438–43.
[27] Fujino T, Nomoto H, Kutsuna S, Ujiie M, Suzuki T, Sato R, et al. Novel SARS-CoV-2 variant in travelers from Brazil to Japan. *Emerg Infect Dis* 2021;27:1243–5.
[28] Xia S, Wang L, Zhu Y, Lu L, Jiang S. Origin, virological features, immune evasion and intervention of SARS-CoV-2 Omicron sublineages. *Signal Transduct Targeted Ther* 2022;7:241.
[29] Yu J, Collier AY, Rowe M, Mardas F, Ventura JD, Wan H, et al. Neutralization of the SARS-CoV-2 omicron BA.1 and BA.2 variants. *N Engl J Med* 2022;386:1579–80.
[30] Bruel T, Hadjadj J, Maes P, Planas D, Seve A, Staropoli I, et al. Serum neutralization of SARS-CoV-2 Omicron sublineages BA.1 and BA.2 in patients receiving monoclonal antibodies. *Nat Med* 2022;28:1297–302.
[31] Lusvarghi S, Pollett SD, Neerukonda SN, Wang W, Wang R, Vassell R, et al. SARS-CoV-2 BA.1 variant is neutralized by vaccine booster-elicited serum but evades most convalescent serum and therapeutic antibodies. *Sci Transl Med* 2022;14:eabn8543.
[32] Tada T, Zhou H, Dcosta BM, Samanovic MI, Chivukula V, Herati RS, et al. Increased resistance of SARS-CoV-2 Omicron variant to neutralization by vaccine-elicited and therapeutic antibodies. *eClinicalMedicine* 2022;78:103944.
[33] Hoffmann M, Krüger N, Schulz S, Cossmann A, Rocha C, Kempf A, et al. The Omicron variant is highly resistant against antibody-mediated neutralization: implications for control of the COVID-19 pandemic. *Cell* 2022;185:447–456.e11.
[34] Liu L, Iketani S, Guo Y, Chan JF, Wang M, Liu L, et al. Striking antibody evasion manifested by the Omicron variant of SARS-CoV-2. *Nature* 2022;602:676–81.
[35] Ng KW, Faulkner N, Cornish GH, Rosa A, Harvey R, Hussain S, et al. Preexisting and de novo humoral immunity to SARS-CoV-2 in humans. *Science* 2020;370:1339–43.
[36] Pinto D, Sauer MM, Czudnochowski N, Low JS, Tortorici MA, Housley MP, et al. Broad betacoronavirus neutralization by a stem helix-specific human antibody. *Science* 2021;373:1109–16.

[37] Sauer MM, Tortorici MA, Park YJ, Walls AC, Homad L, Acton OJ, et al. Structural basis for broad coronavirus neutralization. *Nat Struct Mol Biol* 2021;28:478–86.
[38] Zhou P, Yuan M, Song G, Beutler N, Shaabani N, Huang D, et al. A human antibody reveals a conserved site on beta-coronavirus spike proteins and confers protection against SARS-CoV-2 infection. *Sci Transl Med* 2022;14:eabi9215.
[39] Chi X, Yan R, Zhang J, Zhang G, Zhang Y, Hao M, et al. A neutralizing human antibody binds to the N-terminal domain of the spike protein of SARS-CoV-2. *Science* 2020;369:650–5.
[40] Cao Y, Yisimayi A, Jian F, Song W, Xiao T, Wang L, et al. BA.2.12.1, BA.4 and BA.5 escape antibodies elicited by Omicron infection. *Nature* 2022;608:593–602.
[41] Desingu PA, Nagarajan K, Dhama K. Emergence of Omicron third lineage BA.3 and its importance. *J Med Virol* 2022;94:1808–10.
[42] Tegally H, Moir M, Everatt J, Giovanetti M, Scheepers C, Wilkinson E, et al. Emergence of SARS-CoV-2 omicron lineages BA.4 and BA.5 in South Africa. *Nat Med* 2022;28:1785–90.
[43] Kurhade C, Zou J, Xia H, Liu M, Chang HC, Ren P, et al. Low neutralization of SARS-CoV-2 Omicron BA.2.75.2, BQ.1.1 and XBB.1 by parental mRNA vaccine or a BA.5 bivalent booster. *Nat Med* 2023;29:344–7.
[44] Uraki R, Kiso M, Iwatsuki-Horimoto K, Yamayoshi S, Ito M, Chiba S, et al. Characterization of a SARS-CoV-2 EG.5.1 clinical isolate *in vitro* and *in vivo*. *Cell Rep* 2023;42:113580.
[45] Khan K, Lustig G, Römer C, Reedoy K, Jule Z, Karim F, et al. Evolution and neutralization escape of the SARS-CoV-2 BA.2.86 subvariant. *Nat Commun* 2023;14:8078.
[46] Graham BS, Gilman MSA, McLellan JS. Structure-based vaccine antigen design. *Annu Rev Med* 2019;70:91–104.
[47] Dreyfus C, Laursen NS, Kwaks T, Zuijdgeest D, Khayat R, Ekiert DC, et al. Highly conserved protective epitopes on influenza B viruses. *Science* 2012;337:1343–8.
[48] Corti D, Lanzavecchia A. Broadly neutralizing antiviral antibodies. *Annu Rev Immunol* 2013;31:705–42.
[49] Flyak AI, Kuzmina N, Murin CD, Bryan C, Davidson E, Gilchuk P, et al. Broadly neutralizing antibodies from human survivors target a conserved site in the Ebola virus glycoprotein HR2-MPER region. *Nat Microbiol* 2018;3:670–7.
[50] Ma W, Yang J, Fu H, Su C, Yu C, Wang Q, et al. Genomic perspectives on the emerging SARS-CoV-2 omicron variant. *Dev Reprod Biol* 2022;20:60–9.
[51] Jin X, Zhou W, Luo M, Wang P, Xu Z, Ma K, et al. Global characterization of B cell receptor repertoire in COVID-19 patients by single-cell V(D)J sequencing. *Briefings Bioinf* 2021;22:bbab192.
[52] Jaimes JA, André NM, Chappie JS, Millet JK, Whittaker GR. Phylogenetic analysis and structural modeling of SARS-CoV-2 spike protein reveals an evolutionary distinct and proteolytically sensitive activation loop. *J Mol Biol* 2020;432:3309–25.
[53] Hu J, Chen X, Lu X, Wu L, Yin L, Zhu L, et al. A spike protein S2 antibody efficiently neutralizes the Omicron variant. *Cell Mol Immunol* 2022;19:644–6.
[54] Huang KA, Tan TK, Chen TH, Huang CG, Harvey R, Hussain S, et al. Breadth and function of antibody response to acute SARS-CoV-2 infection in humans. *PLoS Pathog* 2021;17:e1009352.
[55] Reuter N, Chen X, Kropff B, Peter AS, Britt WJ, Mach M, et al. SARS-CoV-2 spike protein is capable of inducing cell-cell fusions independent from its receptor ACE2 and this activity can Be impaired by furin inhibitors or a subset of monoclonal antibodies. *Viruses* 2023;15:1500.
[56] Park SB, Khan M, Chiliveri SC, Hu X, Irvin P, Leek M, et al. SARS-CoV-2 omicron variants harbor spike protein mutations responsible for their attenuated fusogenic phenotype. *Commun Biol* 2023;6:556.
[57] Fan X, Cao D, Kong L, Zhang X. Cryo-EM analysis of the post-fusion structure of the SARS-CoV spike glycoprotein. *Nat Commun* 2020;11:3618.
[58] Lip KM, Shen S, Yang X, Keng CT, Zhang A, Oh HL, et al. Monoclonal antibodies targeting the HR2 domain and the region immediately upstream of the HR2 of the S protein neutralize *in vitro* infection of severe acute respiratory syndrome coronavirus. *J Virol* 2006;80:941–50.
[59] Elshabrawy HA, Coughlin MM, Baker SC, Prabhakar BS. Human monoclonal antibodies against highly conserved HR1 and HR2 domains of the SARS-CoV spike protein are more broadly neutralizing. *PLoS One* 2012;7:e50366.
[60] Mikulska M, Sepulcri C, Dentone C, Magne F, Balletto E, Baldi F, et al. Triple combination therapy with 2 antivirals and monoclonal antibodies for persistent or relapsed severe acute respiratory syndrome coronavirus 2 infection in immunocompromised patients. *Clin Infect Dis* 2023;77:280–6.
[61] Levin MJ, Ustianowski A, De Wit S, Launay O, Avila M, Templeton A, et al. Intramuscular AZD7442 (Tixagevimab-Cilgavimab) for prevention of COVID-19. *N Engl J Med* 2022;386:2188–200.
[62] Tuekprakhon A, Nutalai R, Dijokaite-Guraliuc A, Zhou D, Ginn HM, Selvaraj M, et al. Antibody escape of SARS-CoV-2 Omicron BA.4 and BA.5 from vaccine and BA.1 serum. *Cell* 2022;185:2422–2433.e13.
[63] Faraone JN, Qu P, Goodarzi N, Zheng YM, Carlin C, Saif LJ, et al. Immune evasion and membrane fusion of SARS-CoV-2 XBB subvariants EG.5.1 and XBB.2.3. *Emerg Microb Infect* 2023;12:2270069.
[64] Zhang S, Zhang H, Ghia EM, Huang J, Wu L, Zhang J, et al. Inhibition of chemotherapy resistant breast cancer stem cells by a ROR1 specific antibody. *Proc Natl Acad Sci USA* 2019;116:1370–7.
[65] Colovos C, Yeates TO. Verification of protein structures: patterns of nonbonded atomic interactions. *Protein Sci* 1993;2:1511–9.
[66] Eisenberg D, Lüthy R, Bowie JU. VERIFY3D: assessment of protein models with three-dimensional profiles. *Methods Enzymol* 1997;277:396–404.
[67] Ramachandran GN, Ramakrishnan C, Sasisekharan V. Stereochemistry of polypeptide chain configurations. *J Mol Biol* 1963;7:95–9.
[68] Sali A, Blundell TL. Comparative protein modelling by satisfaction of spatial restraints. *J Mol Biol* 1993;234:779–815.